NUKLEONIKA 2017;62(2):177–181
doi: 10.1515/nuka-2017-0027

ORIGINAL PAPER

DE GRUYTER OPEN

© 2017 Agata Stoch *et al*. This is an open access article distributed under the Creative Commons Attribution -NonCommercial-NoDerivatives 3.0 License (CC BY-NC-ND 3.0).

# Crystal structure and Mössbauer effect in multiferroic $0.5BiFeO_3$-$0.5Pb(Fe_{0.5}Ta_{0.5})O_3$ solid solution

**Agata Stoch, Jan Maurin, Paweł Stoch, Jan Kulawik, Dorota Szwagierczak**

**Abstract.** Multiferroic $0.5BiFeO_3$-$0.5Pb(Fe_{0.5}Ta_{0.5})O_3$ solid solution is a material that exhibits ferroelectric and antiferromagnetic orderings in ambient temperature. The solid solution was obtained as a result of a conventional reaction in a solid state. The obtained material is a dense, fine-grained sinter whose surface was observed by scanning electron microscopy (SEM) and stoichiometry was confirmed by energy dispersive X-ray spectroscopic (EDS) analysis. According to the X-ray powder diffraction (XRD) measurements, the main phase is *R*3*c* space group with admixture of *Pm*-3*m* regular phase. Small contribution of pyrochlore-like phase was also observed. Mössbauer spectroscopy suggested random distribution of $Fe^{3+}/Ta^{5+}$ cations in the B sites of $ABO_3$ compound. Reduction of the magnetic hyperfine field with an increase in the substitution of $Ta^{5+}$ in $Fe^{3+}$ neighbourhood was also observed.

**Keywords:** $BiFeO_3$ • crystal structure • hyperfine interactions • multiferroics • solid solution

A. Stoch✉, J. Kulawik, D. Szwagierczak
Institute of Electron Technology Krakow Division,
39 Zabłocie Str., 30-701 Kraków, Poland,
Tel.: +48 12 656 3144 ext. 265, Fax: +48 12 656 3626,
E-mail: agata.stoch@gmail.com

J. Maurin
National Centre for Nuclear Research,
7 Sołtana Str., 05-400 Otwock/Świerk, Poland
and National Medicines Institute,
30/34 Chełmska Str., 00-725 Warsaw, Poland

P. Stoch
Faculty of Materials Science and Ceramics,
AGH University of Science and Technology,
30 Mickiewicza Ave., 30-059 Kraków, Poland

Received: 26 June 2016
Accepted: 2 October 2016

## Introduction

Materials that exhibit ferromagnetic and ferroelectric ordering in the same phase are named magnetoelectrics, which are part of a larger group of multiferroics. Multiferroics possess at least two ferroic orderings at the same time. Magnetoelectric materials are characterized by a strong coupling between the magnetic and electric subsystems, which means that the magnetic field is able to induce electric polarization and *vice versa*.

The first single-phase multiferroic perovskite oxides ($ABO_3$) were discovered in early 1960s. However, very limited progress has been made during the past several decades [1–6]. The significant development of multiferroic materials started with the successful synthesis of multiferroic thin films [7].

Magnetoelectrics are widely used as transducers, actuators, detectors, and other sensors that are characterized by high dielectric permittivity and magnetic permeability [1–7]. Strong coupling between electrical polarization and magnetization vectors is desirable for a new class of multifunctional materials, for example, new mass storage devices. Unfortunately, most multiferroic materials are characterized by a low magnetic ordering temperature, considerably below room temperature, what limits their practical applications.

Bismuth ferrite ($BiFeO_3$) is a well-known perovskite compound that simultaneously exhibits

ferroelectric ($T_C$ = 1110 K) and antiferromagnetic ($T_N$ = 610 K) orderings at ambient temperature. The stereochemical activity of Bi lone-pair electrons induces ferroelectric polarization, while the partially filled 3*d* orbitals of the $Fe^{3+}$ ions produce G-type antiferromagnetic ordering. $BiFeO_3$ has a spatially modulated magnetic structure of a cycloidal type with a period of modulation of about 62 nm [4, 7]. One way to suppress the spiral spin modulation is the chemical substitution of magnetically active atoms, especially rare earth trivalent ions, into the Bi sublattice [4].

Lead iron tantalate ($Pb(Fe_{0.5}Ta_{0.5})O_3$) is another type of magnetoelectric material where ferroelectrically active $Ta^{5+}$ cations are partially substituted by magnetic $Fe^{3+}$ ions of a different valence state, the so-called paramagnetic substitution [5]. As a consequence, $Pb(Fe_{0.5}Ta_{0.5})O_3$ exhibits antiferromagnetic ordering at temperatures below 130–180 K as well as ferroelectric ordering at temperature below 270 K [8–12]. It is considered that the magnetic ordering temperature and magnetic properties of the iron-containing oxides depend on the number of Fe-O-Fe linkages in a crystal lattice [13]. The number of Fe-O-Fe linkages can be governed by changing the $Ta^{5+}/Fe^{3+}$ ratio and/or the degree of $Fe^{3+}$ and $Ta^{5+}$ cations ordering. However, no such ordering have been observed and $Pb(Fe_{0.5}Ta_{0.5})O_3$ could be considered as a fully disordered in B-site sublattice of perovskite structure [8–10]. On the other hand, for a similar $Pb(Fe_{0.5}Nb_{0.5})O_3$ compound, large scattering of magnetic ordering temperature could be explained by local compositional ordering and formation of Nb-poor-Fe-rich and Nb-rich-Fe-poor regions as postulated in [14–16]. Additionally, $Pb(Fe_{0.5}Ta_{0.5})O_3$ is a perovskite relaxor, is reported to have a very high dielectric constant, and can be used as a multilayer ceramic capacitor [17].

The $0.5BiFeO_3$-$0.5Pb(Fe_{0.5}Ta_{0.5})O_3$ solid solution is a mixture of two compounds in which multiferroicity is governed by two different mechanisms such as lone pairs in $BiFeO_3$ and paramagnetic substitution of $Fe^{3+}$ cations by ferroelectrically active $Ta^{5+}$, although the lone pairs mechanism could not be excluded in $Pb(Fe_{0.5}Ta_{0.5})O_3$ [18]. In this paper, we report the synthesis, crystal structure, and hyperfine interactions in $0.5BiFeO_3$-$0.5Pb(Fe_{0.5}Ta_{0.5})O_3$ solid solution. The aim of the research was to find the correlation between the structure and the size of hyperfine interactions.

## Experimental

High-purity $Bi_2O_3$, PbO, $Fe_2O_3$, and $Ta_2O_5$ oxide powders were weighted in stoichiometric proportions, mechanically activated for 7 h during a ball milling process, pressed into pellets, and calcined at 1093 K for 4 h. The molder was then granulated and pressed into a disc-shaped pellet. The pellets were heat treated at 818 K for 2 h and then sintered at 1123 K for 10 h. The pellets were then cooled down to room temperature with the rate of cooling of the furnace.

Crystal structure of the powdered material was checked by Bruker-AXS D8 diffractometer in the Bragg-Brentano geometry at room temperature using $CuK_\alpha$ radiation of wave length $\lambda$ = 1.5418 Å.

The surface of the fractured sample was observed by scanning electron microscopy (SEM) using FEI Nova NanoSEM 200 equipped with energy dispersive X-ray spectroscopy (EDS) by EDAX company.

Transmission $^{57}Fe$ Mössbauer spectroscopy measurements were performed on a WissEl spectrometer with Oxford cryostat at 77 K. The spectrometer was calibrated using ARMCO foil at room temperature and all isomer shift (IS) values are related to this standard. Share of the particular components was estimated by assuming the same value of Lamba-Mössbauer parameter.

## Results and discussion

### SEM-EDS studies

Surface of the $0.5BiFeO_3$-$0.5Pb(Fe_{0.5}Ta_{0.5})O_3$ ceramic sample is presented in Fig. 1. The material is a fine-grained, dense sinter with small grains of few micrometres in size. Energy dispersive analysis was performed at various points corresponding to larger and smaller grains. The EDS profile analysis is close to the theoretical oxide composition within the experimental error range in points 1 and 2 (Fig. 1). In case of point 3, in which the grain size is the smallest, there is a lower concentration of iron. There are no unreacted starting oxides and phases, which can be precipitated as a result of a possible evaporation of $Bi_2O_3$ and PbO during the synthesis process.

### Crystal structure

Crystal structure and phase purity of the sinter were checked by X-ray powder diffraction (XRD). A fitting program (FullProf software [19]), based on the Rietveld method, was used to analyse the diffraction pattern.

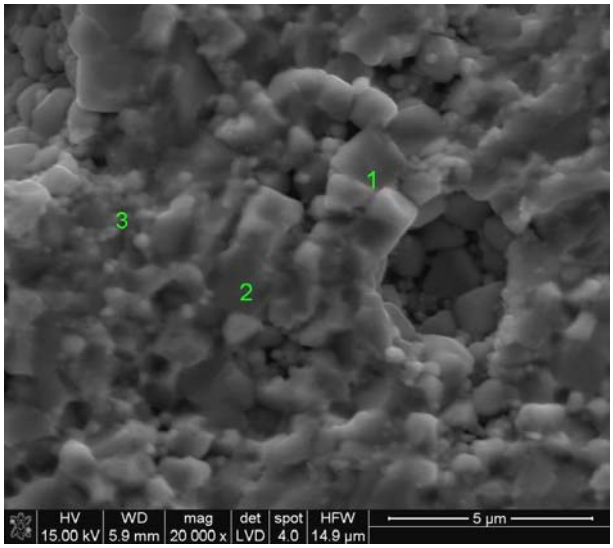


**Fig. 1.** SEM image of $0.5BiFeO_3$-$0.5Pb(Fe_{0.5}Ta_{0.5})O_3$.

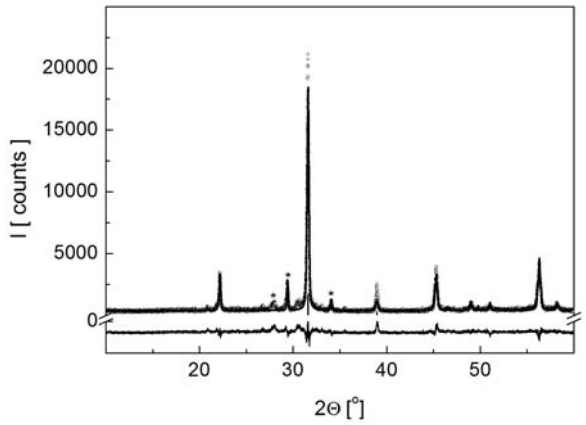


**Fig. 2.** XRD pattern of $0.5BiFeO_3$-$0.5Pb(Fe_{0.5}Ta_{0.5})O_3$. The impurity pyrochlore phase is represented by asterisks.

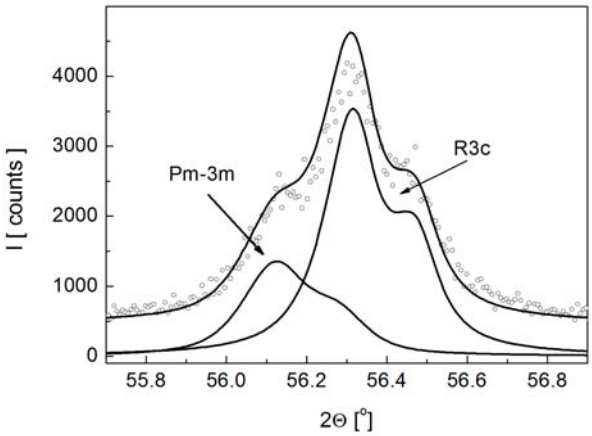


**Fig. 3.** The Bragg reflex of the studied solid solution at approximately 56.3°.

The simple $ABO_3$ perovskite crystallizes in a cubic *Pm*-3*m* crystal structure, although the ferroelectric materials distinctly show an off-centre shift of the B-site cation during polarization ordering, and, therefore, a small tetragonal distortion is observed. Additionally, the coexistence of ferroelectric and ferromagnetic orderings often leads to the rotations of the oxygen octahedra resulting in rhombohedral distortion [18]. The crystallographic transitions are not distinct and, therefore, difficult to measure. A few probable crystal structures such as *Pm*-3*m*, *P*4*mm*, *R*3*c*, and *Cm* were examined during the refinement procedure. The XRD pattern is presented in Fig. 2. The best result was obtained by assuming *R*3*c* space group for the main phase. The lattice parameters of the phase are $a = b = 5.6524(4)$ Å and $c = 13.8489(18)$ Å, and thus the rhombohedral angle is 59.97°, which is close to 60° (the value for a cubic structure in rhombohedral coordinates), thus the observed rhombohedral distortion is very small.

Pure $BiFeO_3$ is formed only when $Bi_2O_3$ to $Fe_2O_3$ ratio is equal 1:1. Small inhomogeneities lead to the formation of Fe reach phase $Bi_2Fe_4O_9$ and/or Bi reach phase $Bi_{40}Fe_2O_{63}$ [20]. Additionally, frequently observed impurity phases are pyrochlores, which could be a solid solution of $(Pb,Bi)_2(Fe,Ta)_2O_7$. In the obtained material, the pyrochlore phase was also added during the fitting procedure and is represented by asterisk in Fig. 2. The fitted secondary phase is similar to pyrochlores of reference codes 00-014-0318 and 00-034-0871 from ICDD database. The quantity of this phase according to the Rietveld refinement is approximately 10 mass%.

The calculated Goldschmidt tolerance factor for the studied solid solution is 0.95, which is close to unity, and thus ideal cubic perovskite structure is privileged. On the other hand, ferroelectrically active cations such as $Pb^{2+}$ and $Ta^{5+}$ enforce distortion of the unit cell but we cannot exclude the existence of the cubic symmetry. Closer look at the Bragg reflex at the higher angle of about 56° showed more complex structure of the peak, which is presented in Fig. 3.

At approximately 56.1°, another peak that originated from the regular cubic phase can be observed. Thus *Pm*-3*m* space group was also added to the fitting procedure. The existence of the cubic centrosymmetric phase excludes possibility of electric and magnetic orderings [18]. Therefore, it could be assumed that the obtained material is in paramagnetic and paraelectric state. On the basis of the EDS analysis, both phases should have a similar stoichiometry. Therefore, we conclude, at this moment, that the $0.5BiFeO_3$-$0.5Pb(Fe_{0.5}Ta_{0.5})O_3$ solid solution is a mixture of two very similar crystal phases. One is a perovskite-like *R*3*c* (about 70 mass%) in which the material could possess magnetic and electric orderings [18]. The second is the regular perovskite *Pm*-3*m* (about 20 mass%) in which, based on the fundamental symmetry consideration, electric and magnetic orderings are forbidden [18].

## Mössbauer spectroscopy

In order to investigate the local crystallochemical environment at atomic scale, Mössbauer spectroscopy was used. A typical transmission spectrum of the obtained solid solution measured at 77 K is presented in Fig. 4. The obtained spectrum is a composition of four Zeeman sextets and two paramagnetic doublets. For the $0.5BiFeO_3$-$0.5Pb(Fe_{0.5}Ta_{0.5})O_3$ compound, the Goldsmith tolerance factor is smaller than unity, what suggests random distribution of $Fe^{3+}/Ta^{5+}$ cations at the B site of the $ABO_3$ perovskite structure. In the perovskite, every iron octahedron is neighboured

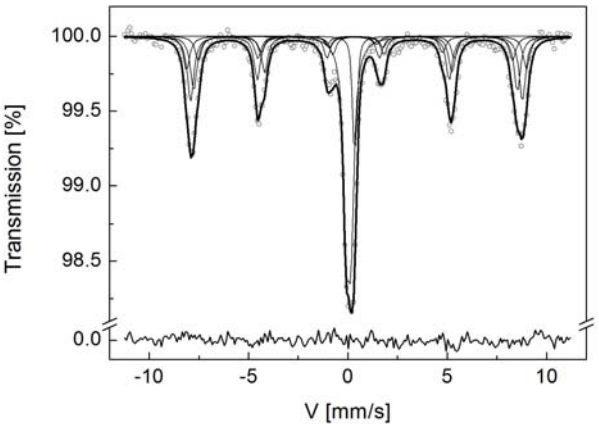


**Fig. 4.** $^{57}Fe$ Mössbauer spectrum of the $0.5BiFeO_3$-$0.5Pb(Fe_{0.5}Ta_{0.5})O_3$ solid solution at 77 K.

**Table 1.** The hyperfine interaction parameters of the $0.5BiFeO_3$-$0.5Pb(Fe_{0.5}Ta_{0.5})O_3$ solid solution at 77 K

| Compound no. | *A* [%] | IS [mm/s] | $\mu_0 H_{hf}$ [T] | QS [mm/s] |
|---|---|---|---|---|
| 1 | 12.0 | 0.53(1) | 52.98(1) | 0.01(1) |
| 2 | 23.4 | 0.46(1) | 51.72(2) | 0.08(1) |
| 3 | 19.6 | 0.56(1) | 50.45(2) | –0.07(1) |
| 4 | 8.9 | 0.39(1) | 48.97(3) | 0.09(1) |
| 5 | 29.3 | 0.15(1) | 0 | 0.12(1) |
| 6 | 6.8 | 0.46(1) | 0 | 0.06(1) |

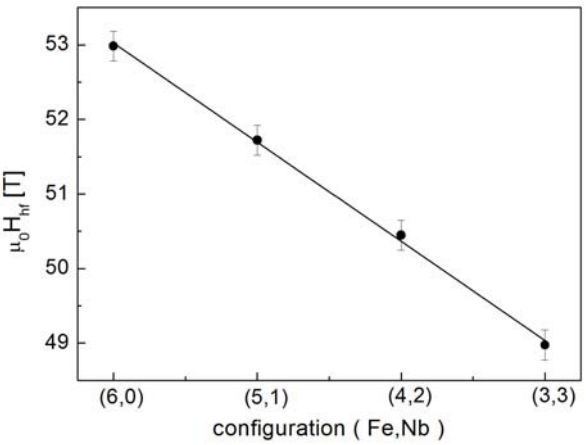


**Fig. 5.** The magnetic hyperfine field ($\mu_0 H_{hf}$) dependence of the configuration of atoms in the surrounding octahedrons.

by six other octahedrons; in the middle of each, $Fe^{3+}$ or $Ta^{5+}$ cations are randomly distributed. Therefore, a fitting model based on binomial distribution was used, where $P(6;n) = 6!/[(6-n)!n!]\cdot(1-x)^{6-n}x^n$ is the probability of individual neighbourhood of selected iron atom composed of $(6-n)$ Fe atoms and $(n = 0, 1, 2, ..., 6)$ Ta atoms and $x = 0.25$ corresponds to the stoichiometry of the studied solid solution. Particular neighbourhoods of iron atoms produce the individual subspectra that contribute to the overall Mössbauer effect pattern. Assuming that the areas of particular Mössbauer subspectra follow the probabilities $P(6;n)$, a fitting procedure was performed with a limited number of employed sextets because of the postulation that probabilities below 5% were neglected. Therefore, at a final stage of the fitting procedure, four of the subspectra were considered. This fitting model was used only for magnetically splitted components. The similar fitting procedure was previously used for other perovskite multiferroics [21]. The obtained hyperfine interaction parameters such as area ($A$), isomer shift (IS), magnetic hyperfine field ($\mu_0 H_{hf}$), and quadrupole shift (QS) are summarized in Table 1. For magnetic components subspectra 1–4, weighted mean values were obtained and are as follow: $<IS> = 0.495$ mm/s, $<\mu_0 H_{hf}> = 51.19$ T, $<QS> = 0.022$ mm/s. These mean values are similar to the values obtained previously for comparable multiferroic solid solutions [21, 22].

One of the quadrupole doublets (component no. 5) can be related to the iron in paramagnetic and paraelectric regular phase that was observed on the XRD pattern. The second much smaller one could be ascribed to iron in pyrochlore impurity phase that is also evidenced at the XRD pattern, and the obtained IS value is in the range 0.40–0.49 mm/s, which was previously reported for pyrochlores of similar composition [23].

The use of binominal distribution in fitting of the spectra gives us the possibility to ascribe the magnetically splitted components to the different surroundings of the studied iron nuclei. According to the obtained probabilities, components no. 1–4 (Table 1) could be assigned to the configurations (6,0), (5,1), (4,2) and (3,3), respectively, where the first number in the bracket is the number of surrounded octahedrons with $Fe^{3+}$ in the middle and the second one with $Ta^{5+}$. It can be seen that increasing the number of $Ta^{5+}$ in the local surrounding of iron lead to the reduction of the $\mu_0 H_{hf}$ field. This dependence is presented in Fig. 5 and the linear behaviour is evidenced.

## Conclusions

The $0.5BiFeO_3$-$0.5Pb(Fe_{0.5}Ta_{0.5})O_3$ perovskite was synthesized by means of a conventional solid-state reaction method. The obtained material is a dense, fine-grained sinter. According to the XRD analysis, the main crystal phase is rhombohedral *R*3*c* with the addition of some regular *Pm*-3*m* space group. The Mössbauer spectroscopy confirmed the existence of magnetic ordering of the *R*3*c* structure with a possible random distribution of the $Fe^{3+}/Ta^{5+}$ cations in the unit cell of the $0.5BiFeO_3$-$0.5Pb(Fe_{0.5}Ta_{0.5})O_3$. This substitution decreases the number of Fe-O-Fe linkages, what lead to the decrease in the magnetic hyperfine field.

**Acknowledgments.** The work was partially supported from statutory funds of Institute of Electron Technology Krakow Division in 2016.

## References

1. Scott, J. F. (2007). Data storage: Multiferroic memories. *Nat. Mater.*, *6*, 256–257. DOI: 10.1038/nmat1868.
2. Paik, H., Hwang, H., No, K., Kwon, S., & Cann, D. P. (2007). Room temperature multiferroic properties of single-phase $(Bi_{0.9}La_{0.1})FeO_3$–$Ba(Fe_{0.5}Nb_{0.5})O_3$ solid solution ceramics. *Appl. Phys. Lett.*, *90*, 042908. DOI: 10.1063/1.2434182.
3. Yuan, G. L., Or, S. W., Liu, J. M., & Liu, Z. G. (2006). Structural transformation and ferroelectromagnetic behavior in single-phase $Bi_{1-x}Nd_xFeO_3$ multiferroic ceramics. *Appl. Phys. Lett.*, *89*, 052905. DOI: 10.1063/1.2266992.

4. Zhang, S. T., Zhang, Y., Lu, M. H., Du, C. L., Chen, Y. F., Liu, Z. G., Zhu, Y. Y., Ming, N. B., & Pan, X. Q. (2006). Substitution-induced phase transition and enhanced multiferroic properties of BiLaFeO ceramics. *Appl. Phys. Lett.*, *88*, 162901. DOI: 10.1063/1.2195927.
5. Yang, Y., Liu, J. M., Huang, H. B., Zuo, W. Q., Bao, P., & Liu, Z. G. (2004). Magnetoelectric coupling in ferroelectromagnet $Pb(Fe_{1/2}Nb_{1/2})O_3$ single crystals. *Phys. Rev. B*, *70*, 132101–132105. DOI: 10.1103/PhysRevB.70.132101.
6. Kulawik, J., & Szwagierczak, D. (2007). Dielectric properties of manganese and cobalt doped lead iron tantalate ceramics. *J. Eur. Ceram. Soc.*, *27*, 2281–2286. DOI: 10.1016/j.jeurceramsoc.2006.07.010.
7. Wang, J., Neaton, J. B., Zheng, H., Nagarajan, V., Ogale, S. B., Liu, B., Viehland, D., Vaithyanathan, V., Schlom, D. G., Waghmare, U. V., Spaldin, N. A., Rabe, K. M., Wuttig, M., & Ramesh, R. (2003). Epitaxial $BiFeO_3$ multiferroic thin film heterostructures. *Science*, *299*, 1719–1722. DOI: 10.1126/science.1080615.
8. Lampis, N., Sciau, P., & Lehmann, A. G. (2000). Rietveld refinements of the paraelectric and ferroelectric structures of $PbFe_{0.5}Ta_{0.5}O_3$. *J. Phys.-Condens. Matter*, *12*(11), 2367–2378. DOI: 10.1088/0953-8984/12/11/303.
9. Nomura, S., Takabayashi, H., & Nakagawa, T. (1968). Dielectric and magnetic properties of $Pb(Fe_{1/2}Ta_{1/2})O_3$. *Jpn. J. Appl. Phys.*, *7*, 600–604. DOI: 10.1143/JJAP.7.600.
10. Falqui, A., Lampis, N., Geddo-Lehmann, A., & Pinna, G. (2005). Low temperature magnetic behavior of perovskite compounds $PbFe_{1/2}Ta_{1/2}O_3$ and $PbFe_{1/2}Nb_{1/2}O_3$. *J. Phys. Chem.*, *109*, 22967–22970. DOI: 10.1080/00150193.2014.923682.
11. Martinez, R., Palai, R., Huhtinen, H., Liu, J., Scott, J. F., & Katiyar, R. S. (2010). Nanoscale ordering and multiferroic behavior in $PbFe_{1/2}Ta_{1/2}O_3$. *Phys. Rev. B*, *82*, 134104-1–134104-134110. DOI: 10.1103/PhysRevB.82.134104.
12. Kubrin, S. P., Raevskaya, S. I., Kuropatkina, S. A., Raevski, I. P., & Sarychev, D. A. (2006). Dielectric and Mössbauer studies of B-cation order–disorder effect on the properties of $Pb(Fe_{1/2}Ta_{1/2})O_3$ relaxorferroelectric. *Ferroelectrics*, *340*, 155–159. DOI: 10.1080/00150190600889239.
13. Gilleo, M. A. (1960). Superexchange interaction in ferromagnetic garnets and spinels which contain randomly incomplete linkages. *J. Phys. Chem. Solids*, *13*, 33–39. DOI: 10.1016/0022-3697(60)90124-4.
14. Kleemann, W., Shvartsman, V. V., Borisov, P., & Kania, A. (2010). Coexistence of antiferromagnetic and spin cluster glass order in the magnetoelectric relaxor multiferroic $PbFe_{0.5}Nb_{0.5}O_3$. *Phys. Rev. Lett.*, *105*, 257202-1–257202-4. DOI: 10.1103/PhysRevLett.105.257202.
15. Raevski, I. P., Kubrin, S. P., & Raevskaya, S. I. (2012). Magnetic properties of $PbFe_{1/2}Nb_{1/2}O_3$: Mössbauer spectroscopy and first principles calculations. *Phys. Rev. B*, *85*, 224412-1–224412-5. DOI: 10.1103/PhysRevB.85.224412.
16. Laguta, V. V., Rosa, J., & Jastrabik, L. (2010). $^{93}Nb$ NMR and $Fe^{3+}$ EPR study of local magnetic properties of disordered magnetoelectric $PbFe_{1/2}Nb_{1/2}O_3$. *Mater. Res. Bull.*, *45*, 1720–1727. DOI: 10.1016/j.materresbull.2010.06.060.
17. Kulawik, J., & Szwagierczak, D. (2007). Dielectric properties of manganese and cobalt doped lead iron tantalate ceramics. *J. Eur. Ceram. Soc.*, *27*, 2281–2286. DOI: 10.1016/j.jeurceramsoc.2006.07.010.
18. Wang, K. F., Liu, J. M., & Ren, Z. F. (2009). Multiferroicity. The coupling between magnetic and polarization. *Adv. Phys.*, *58*, 321–448. DOI: 10.1080/00018730902920554.
19. Rodríguez-Carvajal, J. (1993). Recent advances in magnetic structure determination by neutron powder diffraction. *Physica B*, *192*, 55–69. DOI: 10.1016/0921-4526(93)90108-I.
20. Lu, J., Qiao, L. J., Fu, P. Z., & Wu, Y. C. (2011). Phase equilibrium of $Bi_2O_3$-$Fe_2O_3$ pseudo-binary system and growth of $BiFeO_3$ single crystal. *J. Cryst. Growth*, *318*, 936–941. DOI: 10.1016/j.jcrysgro.2010.10.181.
21. Zachariasz, P., Stoch, A., Stoch, P., & Maurin, J. (2013). Hyperfine interactions in $xBi_{0.95}Dy_{0.05}FeO_3$-$(1\text{-}x)Pb(Fe_{2/3}W_{1/3})O_3$ multiferroics. *Nukleonika*, *58*(1), 53–56.
22. Ivanov, S. A., Nordblad, P., Tellgren, R., Ericsson, T., & Rundlof, H. (2007). Structural, magnetic and Mössbauer spectroscopic investigations of the magnetoelectric relaxor $Pb(Fe_{0.6}W_{0.2}Nb_{0.2})O_3$. *Solid State Sci.*, *9*, 440–450. DOI: 10.1016/j.solidstatesciences.2007.03.018.
23. Blanco, M. C., Franco, D. G., Jalit, Y., Pannunzio Miner, E. V., Berndt, G., Paesano Jr., A., Nieva, G., & Carbonio, R. I. E. (2012). Synthesis, magnetic properties and Mössbauer spectroscopy for the pyrochlore family $Bi_2BB'O_7$ with B = Cr and Fe and B' = Nb, Ta and Sb. *Physica B*, *407*, 3078–3080. DOI: 10.1016/j.physb.2011.12.029.